Determination of Concrete Structural Defects by Infrared Spectrum Analysis

A. Gailius, D. Žukauskas⁎

Dept. of Building Materials, Vilnius Gediminas Technical University, Saulėtekio 11, LT-2040 Vilnius, Lithuania

After loading, various damages and air inclusions are formed in the structure of concrete. It is natural that these changes have an influence on the thermal properties of concrete. The aim of this investigation was to find the relationship between different percentage of damage and temperature distribution in concrete after heating. The influence of different damage on temperature distribution in concrete was determined. Infrared spectrum analysis was used for determination of temperature distribution. This method is based on the principle that subsurface anomalies in a material result in localized differences in surface temperature caused by different rates of heat transfer at the defect zones. Three specimens for every percentage of damage were used for each determination of temperature distribution. The specimens were heated, and at the same time it was observed the heat transfer and heat distribution in concrete specimens. Results of the experiment show that infrared spectrum can be used in early stages concrete damage detection.
Keywords: compressive strength, concrete, damage, non-destructive testing, heat transfer, temperature distribution, infrared spectrum.

1. INTRODUCTION

Portland cement concrete is a composite material made up of the hydrated cement matrix, fine aggregate, and coarse aggregate. A major factor determining the strength of the material is the bond at the interface of the matrix and the aggregates [1, 2, 3]. This factor has big influences on character and evolution of concrete cracking [3].

This paper focuses on detecting damages in Portland cement concrete using temperature variation detection by infrared (IR) spectrum analysis. Concrete structure may be damaged due to construction errors, environmental exposure, and service loads. One of the major problems of concrete is cracking as a result of service loads. These damages should be non-destructively detected and characterized in a timely and reliable fashion.

In recent years, numerous studies have been reported giving application examples of non-destructive testing techniques when detecting and locating anomalies in concrete. Scarcity of funds needed for repair or replacement of all structurally deficient or functionally obsolete concrete structures forces the state agencies to search for advanced non-destructive testing (NDT) techniques which will facilitate rapid, cost efficient and reliable condition assessment of existing infrastructure to ensure public safety [4]. Incorporation of the quantitative results of NDT techniques in infrastructure management systems is expected to provide the needed feedback in monitoring for detection and identification of deficiencies, and setting up priorities for repair, retrofitting or replacement actions. Infrared thermography can be used to locate and determine the extent of voids in concrete [4]. However, the heat transfer mechanism pertaining to the detection process has not theoretically been analysed. It is necessary to simulate the detection process by applying an appropriate physical model based on the real phenomena [5]. Temperature variation detection can help test that

physical model.

A task of current paper is to analyse relationship between damages and temperature distribution in concrete.

2. MATERIALS AND EXPERIMENTAL PROCEDURE

For making concrete Ordinary Portland Cement, class 42.5N, Blue Circle, UK was used. Properties of the cement are prescribed by British Standard [6]. The coarse aggregate was manufactured from limestone, Aber Kenfic, Quarry. British Standard [7] and researches [8, 9] prescribe the aggregate properties. The sand was dredged from Bristol Channel, therefore it includes some salt. Generally, sand from the seabed washed even in seawater does not contain harmful quantities of salt. The salt content is limited by British Standard [10]. The sand also contains seashells. This usually has no adverse effect on strength but workability of concrete is slightly reduced. British Standard [11]. Sand was sieved by hand through 1.18 mm sieve before using.

Dry materials for producing four $100 \times 100 \times 500$ mm size beams were thoroughly mixed in CUMFLOW H1–KO4-1526 mixer for 2 min before slowly adding the calculated amount of water. Intermittent hand mixing with hand trowels was necessary to achieve a homogeneous mix. After 5 min of mixing a slump test was carried out for establishing the workability.

The slump test is prescribed in British Standard [12]. The mould for the slump test was a frustum of a cone, 300 mm high. It was placed on a smooth surface with the smaller opening at the top, and filled with concrete in three layers. Each layer was tamped 25 times with a standard 16 mm diameter steel rod, rounded at the end, and the top of surface was struck off. The cone was firmly held against its base during the entire operation; this was facilitated by handles or footrests brazed to the mould. Immediately after filling, the cone was slowly lifted, and then the unsupported concrete slumped. The decrease was measured to "displaced original center". In order to reduce the influence

---

⁎Corresponding author. Tel.: + 370-614-61736; fax.: + 370-5-2700494.
E-mail address: *dangyrasz@hotmail.com* (D. Žukauskas)

on a slump of the variation in the surface friction, the inside of the mould and its base were moistened at the beginning of every test. Prior to lifting of the mould, the area immediately around the base of the cone was cleaned of concrete, which may have dropped accidentally. When mix had a zero slump the water was added to obtain a slump within the 30 – 60 mm, mixed again for 3 – 5 min. and the test repeated. 30 mm of a slump was obtained. Amount of materials required for workability test and slump results are displayed in Table 1.

Concrete beams were cast in $100 \times 100 \times 500$ mm. steel moulds previously assembled and oiled and placed on a vibration table. Vibration was done immediately after placing the concrete.

To achieve the highest possible density of the concrete the mortar was vibrated on a vibrating table. Vibration was applied uniformly to the entire concrete mass, as otherwise some parts of it would be not fully compacted while others might be segregated due to over-vibration. In order to obtain the concrete with identical properties, all moulds were filled and vibrated together at the same time.

Table 1. Amount of materials

Parameters	Amount
Water, kg	4.2
Portland cement, kg	7.6
Sand, kg	15.2
Coarse aggregate, kg	30.4

All moulds were cast at the same time. The specimens were remolded at the age of one day after casting, the specimens were immersed in a water bath for 28 days prior to testing for compressive strength (CS). The temperature of water was $20 \pm 1\,°C$. The temperature of curing water could not be much lower than that of the concrete in order to avoid thermal shock or steep temperature gradients; ACI 308-92 recommends a maximum difference of 11 ºC.

Cylindrical specimens of 42×81 mm (Fig. 1) for thermal conductivity tests were cut from concrete beams of $100 \times 100 \times 500$ mm after the curing period. For specimens cutting Radial Drill R3, Qualters & Smith, UK was used.
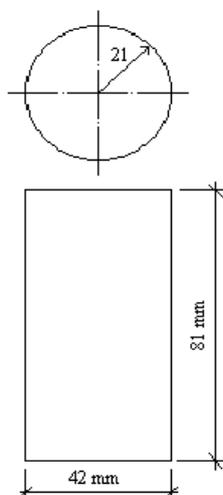
Fig. 1. Specimen for thermal conductivity tests

The CS of concrete was obtained using the standard method prescribed in British Standard [13]. Specimens were crushed by loading them at a constant rate of stress increase of $18\,\text{N\,mm}^{-2}\,\text{min}^{-1}$. Nine cylindrical specimens were used for CS test. Results of CS test are listed in Table 2. Others specimens were compressed with different percentage of CS (35 %, 50 %, 75 %). Results are presented in Table 3.

Table 2. Compressive strength of cylindrical specimens

Number of specimen	Compressive strength F, MN/m^2	Average of compressive strength, MN/m^2
1	34.58	
2	31.19	
3	41.66	
4	27.44	
5	30.61	35.00
6	39.42	
7	33.65	
8	40.72	
9	35.74	

Table 3. Compressive load on cylindrical specimens

Number of specimen	Compressive load P, MN/m^2	Average of compressive load, MN/m^2	Percentage, %
35 % compressive load			
1	12.49		
2	12.35	12.18	34.8
3	11.70		
50 % compressive load			
1	17.11		
2	17.62	17.42	49.8
3	17.55		
75 % compressive load			
1	26.35		
2	26.35	26.35	75.3
3	26.35		

Infrared thermography is based on the principle that subsurface anomalies in a material result in localized differences in surface temperature caused by different rates of heat transfer at the detect zones [4].Thermography senses the emission of thermal radiation from the material surface, and produces a visual image from this thermal signal (Fig. 2) which can be related to the size of an internal defect. Most infrared thermography applications use a thermographic camera in conjunction with an infrared-sensitive detector, which images the heat radiation contrasts. Thermographic imaging may involve active or passive sources, e.g. a flash tube or solar radiation [4, 14].

All materials at a temperature above absolute zero continuously emit energy, and the energy thus emitted, called thermal radiation, is transmitted in the space in the form of electromagnetic waves [4, 15].

Fig. 3 shows a schematic illustration of the experimental apparatus for the temperature variation detection using
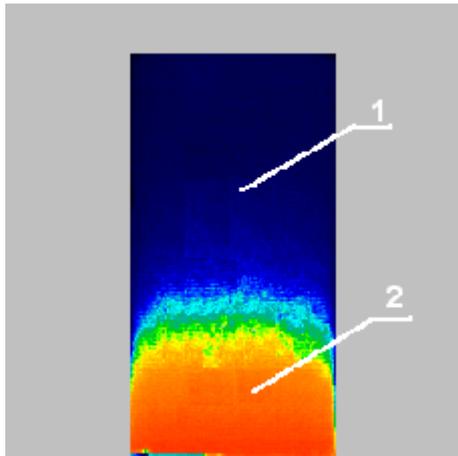
Fig. 2. Visual image of the specimen made by infrared camera (background of image was corrected for better print quality): 1 – low temperature zone; 2 – high temperature zone
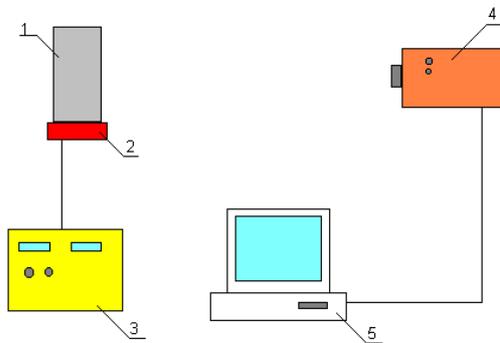
Fig. 3. Schematic illustration of the experimental apparatus for the temperature variation detection using infrared spectrum's analysis: 1 – specimen; 2 – heating element; 3 – powers supply; 4 – IR camera; 5 – computer

infrared spectrum's analysis. As illustrated in Fig. 3, cylindrical specimen was paced vertically on the heating element. Distance between IR camera and specimens surface was 780 mm. For investigating the effect of structural defects on thermophysical properties of concrete by the temperature variation detection using infrared spectrum's analysis, one surface of specimen was heated using heating element (Fig. 3). Temperature of heating element was contorted by power supply. An average of the heating element temperature was $33 \pm 1\,°C$. For the IR images primary analysis computer software Btherm, Version 2.0 for Windows 95/98 was used. The IR spectrums imaging was noted every five minutes. Three specimens with different percentage of damage (0 %, 35 %, 50 % and 75 %) for IR spectrums imaging were used. An average of the ambient temperature was $23 \pm 2\,°C$.

3. RESULTS AND DISCUSSIONS

Concrete can be considered as a highly heterogeneous material because of its composite structure. Various aspects of the behaviour of concrete elements at the rupture limit are explained by this heterogeneity [16].

Coarse aggregates embedded in matrix greatly affect the stress and strain fields, inducing stress concentrations and strain localisation. Furthermore, the interfaces between coarse aggregates and matrix are zones of very high porosity. Therefore, it follows that interface bond microcracks exist in concrete before the load is applied [16, 3]. Experimental investigations have shown how the nature of the stress-strain curve is related to these internal bond cracks [17]. At over 50 % of the ultimate load, the bond cracks begin to increase in length; the load-displacement curve deviates from linearity (Fig. 4).
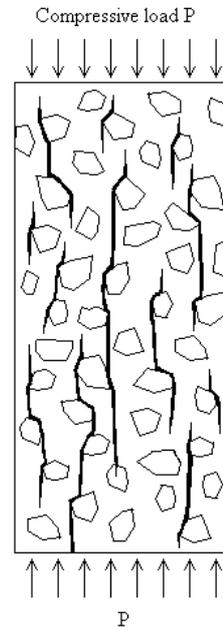
Fig. 4. Development of cracks in concrete

It is natural that changes of sizes; distribution and form of cracks, and porosity have an influence on the thermal properties of concrete. It is known that the size and form of air inclusions have a considerable influence on the thermal properties of hard materials when other parameters are the same [18, 19]. Therefore, we can assume that concrete will have different thermal properties after different loading.

For analysis of IR spectrum images and temperature distribution detection in specimen computer software Btherm, Version 2.0 for Windows 95/98 was used. For errors minimization of determination of temperature variations, temperature readings were done from three lines (Fig. 5). Computer software automatically takes temperature readings from fifty points in every line with 0.1 °C precision. This operation with every IR image was done. These data were used for analysis of temperature distribution in specimens. For this paper data determinate after three hour of heating were used, because during the experimental investigation was observed that thermal conduction processes (temperature distribution in specimens) becomes stable after about three hour. For temperature variation analysis average of temperature difference in specimens after heating (in stabile temperature distribution state) was calculated (Fig. 6). This average can be used as a basis for comparison of temperature distribution in specimens with different percentage of damage (0 %, 35 %, 50 % and 75 %) because this average is the same for all specimens.

Analysis of experimental data shows that after heating appear two separate zones of temperature distribution, i.e.

high temperature zone at bottom of specimen and low temperature zone at top of specimen (Fig. 2). Between these two zones is temperature-sinking zone; this zone can be called temperature gradient (Fig. 6). For determination of top and bottom bounds of temperature gradient we took that temperature differences must be 15 % of maximal and minimal temperatures of specimens. Zones of temperature gradient are less then 20 mm.
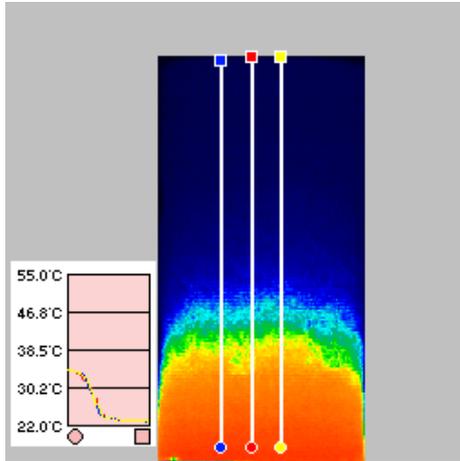
Fig. 5. Infrared spectrum image of the specimen made by infrared camera and finished by computer software (background of image was corrected for better print quality)
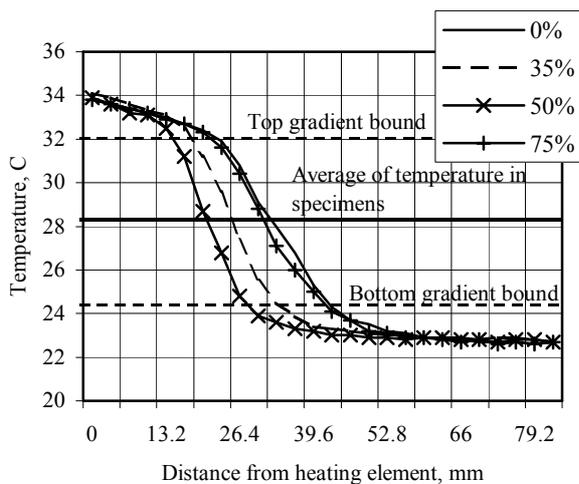
Fig. 6. Temperature distribution in specimens with different percentage of damage after heating

As shown in Fig. 6, temperature distribution in non-damaged specimens and specimens with 75 % of damage is almost the same, i.e. temperature distribution curves are going very similar. The difference between positions of point of average of temperature difference in non-damaged specimen and in specimens with 75 % percentage of damage is only 4.2 %, so small value could be result of determination error. The curves of temperature distribution of specimens with 35 % and 50 % of damage at point of average of temperature difference are going separate. In Table 4 are presented positions of point of average of temperature difference in specimens with different percentage of damage. Reason of it can be character of cracks and heat transfer. As was noted before, at over 50 %

of the ultimate load, the bond cracks begin to increase in length [16, 3], i. e. when load is less than 50 % of the ultimate load generally cracks are growing in zones of, the interfaces between coarse aggregates and matrix. Therefore, it follows that after these loads porosity of concrete is bigger than before. This new value porosity have a big influence on thermal properties of concrete, that can explain separation of temperature gradients of specimens with 35 % and 50 % of damage.

Table 4. Position of point of average of temperature difference in specimens

Variant of gamage	Distance of point of average of temperature difference in specimens from bottom surface of specimen, mm	Difference among positions of point of average of temperature difference in non-damaged specimen and in specimens with different percentage of damage, %
0 %	32.4	–
35 %	24.1	25.6
50 %	20.8	35.8
75 %	30.7	4.2

At over 50 % of the ultimate load, the cracks begin to increase in length and are developing in matrix and coarse aggregates (Fig. 5) almost linearly. The direction of cracks, which are results of loading, is almost the same as direction of this load (Fig. 5) [16, 3]. It is known that cracks almost do not have any influences on thermal properties of concrete when direction of heat transfer is the same as direction of cracks [18]. It can explain why the curve of temperature distribution (Fig. 6) of specimens with 75 % of damage is almost the same as the curve of non-damaged specimens.

Many factors could have influence on results of this investigation, i. e. character of damages in small speci-mens, time of heating, temperature of heating, conditions of experiments, etc. One of these factors is direction of heat transfer. Because of heat diffusion through profile surface the heat transfer direction deviates from linearity (Fig. 7). Temperature distribution in specimens, which we can observe in the infrared spectrum images specimen made by infrared camera also prove the present hypothesis.
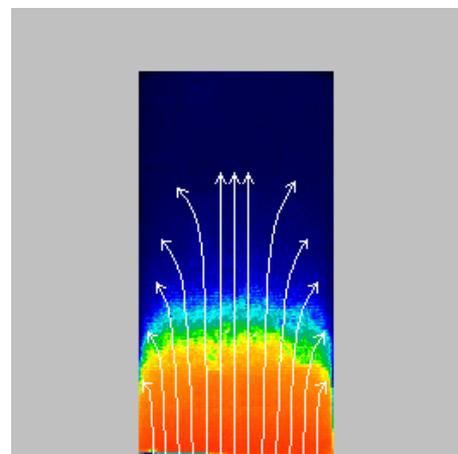
Fig. 7. Heat transfer directions in specimens (background of image was corrected for better print quality)

4. CONCLUSIONS AND RECOMMENDATIONS

1. Experimental investigations showed that with different percentage of damage concrete has different thermal properties, but for final conclusions it is necessary to repeat experiments using larger specimens with more representative structure and specimens with different form, because character of damage depends on the specimen size and form.
2. Results of experiment show that infrared spectrum analysis can be used in early stages of concrete damage.
3. In further researches to get a more presentable results it is necessary to use other non-destructive testing methods together with infrared spectrum analysis, e.g. ultrasonic scan, X-rays, etc.
4. Heating was done in the same direction as loading. Experimental investigations with 90 degrees respect to loading could show different results, because of character of damage and direction of cracks (air inclusions) that are formed in concrete after loading.
5. Experimental data shows that relationship between damages and temperature distribution in concrete specimen exist, and farther investigations on this property of concrete can be useful for NTD techniques evaluation and in future can be as precise method for non-destructive concrete testing.

REFERENCES

1. **Livingston, R. A., Manghnani, M., Prasad, M.** Characterization of Portland Cement Concrete Microstructure Using the Scanning Acoustic Microscope *Cement and Concrete Research* 29 1999: pp. 287 – 291.
2. **Mehta, P. K., Monteiro, P. J. M.** Concrete: Structure, Properties and Materials. Prentice Hall, Englewood Cliffs, 1993.
3. **Zaicev, Y. V.** Modelling of Deformations and Strength of Concrete Using Methods of Destruction Mechanics. Moscow, Stroyizdat, 1982 (in Russian).
4. **Buyukozturk, O.** Imaging of Concrete Structures *NDT & E International* 31 1998: pp. 233 – 243.
5. **Inagaki, T., Ishii, T., Iwamoto, T.** On the NDT and E for the Diagnosis of Defects Using Infrared Thermography *NDT & E International* 32 1999: pp. 247 – 257.
6. British Standard 12: 1996 Spec. for Portland Cements.
7. British Standard 812: Part 1: 1975 Methods for Determination of Particle Size and Shape.
8. **Gailius, A., Vislavičius, K., Žukauskas, D.** Some Optimisation Problems of the Aggregates Composition of Concrete *Proceedings of 6th International Conference "Modern Building Materials, Structures and Techniques" May 19 – 21 1999 Vilnius, Lithuania* 1999: pp. 158 – 162 (in Lithuanian).
9. **Vislavičius, K**. General Principles of Modelling Physical-Mechanical Properties of Conglomerates *Civil Engineering* VI/3 2000: pp. 175 – 178 (in Lithuanian).
10. British Standard 8110: Part 1: 1985 Structural Use of Concrete: Code of Practice for Design and Construction.
11. British Standard 882: 1992 Spec. for Aggregates from Natural Sources for Concrete.
12. British Standard 1881: Part 102: 1983 Method for Determination of Slump.
13. British Standard 1881: Part 116: 1983 Method for Determination of Compressive Strength of Concrete Cubes.
14. **Halmshaw, R.** Non-Destructive Testing, 2nd edn. London, Edward Arnold, 1991.
15. **Ozisik, M. N.** Heat Transfer, a Basic Approach. New York, McGraw Hill, 1985.
16. **Carpinteri, A., Ferro, G., Monetto, I.** Scale Effects in Uniaxially Compressed Concrete Specimens *Magazine of Concrete Research* 51/3 1999: pp. 217 – 225.
17. **Hsu, T., Slate, F. O., Sturman, G. M., Winter, G**. Microcracking of Plain Concrete and the Shape of the Stress-strain Curve *Journal of American Concrete Institute* 60 1963: pp. 209 – 224.
18. **Misnar, A.** Heat Transfer in Solid Materials, Liquids, Gas and their Composites. Moscow, Mir, 1968 (in Russian).
19. **Delpak, R., Gailius, A., Žukauskas, D.** Determination of Thermal-mechanical Properties of Concrete *Journal of Civil Engineering and Management* VIII/2 2002: pp. 121 – 124.